Journal of Applied Polymer Science

Preparation and Property of Poly(vinyl alcohol) Grafted with Butyl Glycidyl Ether

Lixia Wei, Lin Ye
State Key Laboratory of Polymer Materials Engineering, Polymer Research Institute of Sichuan University, Chengdu 610065, China
Correspondence to: L. Ye (E-mail: yelinwh@126.com)

ABSTRACT: The crosslinked polyvinyl alcohol (CPVA) and alkyl chain grafted CPVA (CPVA-*g*-BGE) were prepared through the addition reaction of epoxy group of epichlorohydrin and butyl glycidyl ether (BGE) with the hydroxyl group of PVA. By FTIR and ^{1}HNMR analysis, BGE was confirmed to be grafted onto the molecular chain of PVA successfully. By grafting with BGE, the area of the stress–strain curves of CPVA increased, and the elongation at break increased remarkably with little drop of the tensile strength. Much rougher fractured surface with folds was observed, indicating the increased toughness of CPVA. The relaxation peak corresponding to the glass transition temperature (T_g) of CPVA shifted to low temperature with increasing grafting ratio of BGE. When compared with CPVA, the crystallization ability of CPVA-*g*-BGE decreased, indicating that although the intermolecular hydrogen bonding of PVA was weakened by grafting with alkyl chain, appropriate intermolecular association of alkyl chain facilitated the formation of physical entanglement of molecular chains to strengthen and toughen the PVA matrix. Ink contact angles of CPVA-*g*-BGE decreased with increasing grafting ratio of BGE, indicating the increasing compatibility of CPVA with ink, which was advantageous for PVA to be used as surface sizing agent in papermaking. © 2013 Wiley Periodicals, Inc. J. Appl. Polym. Sci. 129: 3757–3763, 2013

KEYWORDS: properties and characterization; crosslinking; grafting

Received 13 November 2012; accepted 7 February 2013; published online 4 March 2013
DOI: 10.1002/app.39142

INTRODUCTION

Polyvinyl alcohol (PVA) is a polyhydroxy polymer, a synthetic water-soluble resin obtained from hydrolysis of polyvinyl acetate (PVAc),[1,2] which has been widely investigated and applied in coatings, wood and paper adhesives, paper sizing agent, textile, emulsifier, dispersant, oil chemicals, and fibers because of its good biocompatibility, biodegradability, nontoxicity, and environmental friendliness.[3–8] In the papermaking industry, PVA is mainly used in such three areas as beater additives, pigment binders, and surface sizing agent. Surface treatment is applied by paper makers to improve quality of the paper.[9,10] PVA, as an internal or surface sizing agent in papermaking, can be joined with the wood pulp fibers and help to develop the bonded area between the fibers, and the specific forces such as hydrogen bonds holding the fibers together, which would facilitate to improve the strength of the paper product.[11]

To further improve the surface strength and folding endurance of paper, it is important to apply PVA with high strength and toughness as surface sizing agent. Methods of improving the mechanical properties of PVA mainly included plasticizing and compositing. Chang and Kim prepared plasticized PVA by using diethylene glycol as plasticizer, which showed that diethylene glycol imparted toughening effects to PVA film preferably in the range of 10–20 wt % to PVA.[12] Coleman et al. mixed nanotubes with a solution of PVA in water and made films, and showed that, increases in Young's modulus, tensile strength, and toughness of ×3.7, ×4.3, and ×1.7, respectively were observed for the PVA-based materials at less than 1 wt % nanotubes.[13] Chemical crosslinking was also an important method to improve mechanical strength of PVA.[14] Aldehydes, carboxylic acids, anhydrides or acid chlorides, alkoxysilanes, and epichlorohydrin (EPC), etc. were usually used as crosslinking agents. However, the mechanical toughness of PVA would decrease and can not satisfy the application requirement.

In this work, alkyl chain was introduced to molecular chain of PVA during crosslinking process. Through intermolecular entanglement of the alkyl chain and formation of physical crosslinking network, both the strength and toughness of the crosslinked PVA would be expected to be enhanced. The structure and property of the crosslinked PVA grafted with alkyl chain were investigated comprehensively.

EXPERIMENTAL

Materials

PVA (polymerization degree of 1000, hydrolysis degree of 99%) used in this work was a commercial product and supplied by Sichuan Vinylon Co. (China). Butyl glycidyl ether (BGE) with industrial purity was purchased from Shanghai Resin Factory (Shanghai, China) and the epoxy value was 0.5. Sodium hydroxide (NaOH), hydrochloric acid (HCl), and EPC were all of analytically pure and used without further purification.

Synthesis of Crosslinked PVA (CPVA) and BGE Grafted PVA (CPVA-*g*-BEG)

PVA aqueous solution was prepared by fully dissolving 10.0 g of polymer powder without further purification in 90 mL of deionized water, under magnetic stirring in a 250 mL three-necked flask and at temperature of 90°C for 3 h. After cooling to 70°C, EPC (5 wt % of PVA) was quickly added to the PVA aqueous solution, and then NaOH aqueous solution was added drop-wise to the flask. The reaction lasted for about 4 h. The product was neutralized with 20 wt % HCl aqueous solution, washed, and soaked with ethanol and acetone. Finally, the product was dried in vacuum oven at 90°C for 3 h, and the sample of CPVA can be obtained.

As for CPVA-*g*-BEG, BGE was added and mixed homogenously after dissolving PVA, and other process was the same as CPVA.

Measurements

FTIR Analysis. The composition of CPVA samples was analyzed with Nicolet-560 Fourier-transform infrared spectrometer (USA). The specimen was prepared by casting the PVA solution film on KBr discs. The scanning rate is 20 min^{-1}, and the differentiate rate is 4 cm^{-1}.

^{1}H NMR Analysis. ^{1}H NMR measurements of CPVA samples were performed with VARIAN INOVA-400 NMR spectrometer (USA). The aqueous solution of CPVA samples with mass fraction of 5% was prepared. The test was operated at room temperature and a frequency of 400 MHz.

Tensile Testing. The tensile properties of CPVA samples were measured with a 4302 material testing machine from Instron (USA) according to ISO527/1-1993 (E). The sample with dumbbell shape and size of 150 × 10 × 4 mm^3 was prepared. The tensile speed and temperature were 50 mm/min and 23°C, respectively.

SEM Analysis. The fractured surface morphology of CPVA samples was observed with a JEOL JSM-5900LV scanning electron microscope (SEM) (Japan) with an acceleration voltage of 5 kV. The tensile fractured surfaces were sputter-coated with thin layer gold.

DMA Analysis. The dynamic mechanical analysis (DMA) of CPVA samples was carried out with a TA Instrument Q800 DMA (USA). All the samples were measured with a tensile mode over the temperature range of −80 to 100°C at a heating rate of 3°C/min and a frequency of 1 Hz. The sample size was about 40 × 4 × 0.5 mm^3.

Nonisothermal Crystallization Analysis. The nonisothermal crystallization of CPVA samples was performed with a Netzsch 204 Phoenix DSC (Germany). The temperature scale was calibrated with indium. Samples of about 5–10 mg were heated from ambient temperature to 250°C at a constant rate of 40 k/min. After holding for 5 min to eliminate the effect of the previous thermal history, the samples were cooled to ambient temperature at a rate of 10 K/min and then the samples were heated to 250°C with the same constant rate.

The quantity of heat absorbed during melting of the polymer is substantively the quantity of heat for destroying the crystal structure. The higher the crystallinity (X_c), the more the melting heat. X_c can be calculated with the following equation:

$$X_c = (\Delta H_m/\Delta H_0) \times 100\% \quad (1)$$

where ΔH_m is the melting enthalpy of the samples and ΔH_0 is the balanced melting enthalpy, i.e., the melting enthalpy of 100% crystallizing polymer, which is 156 J/g for PVA.

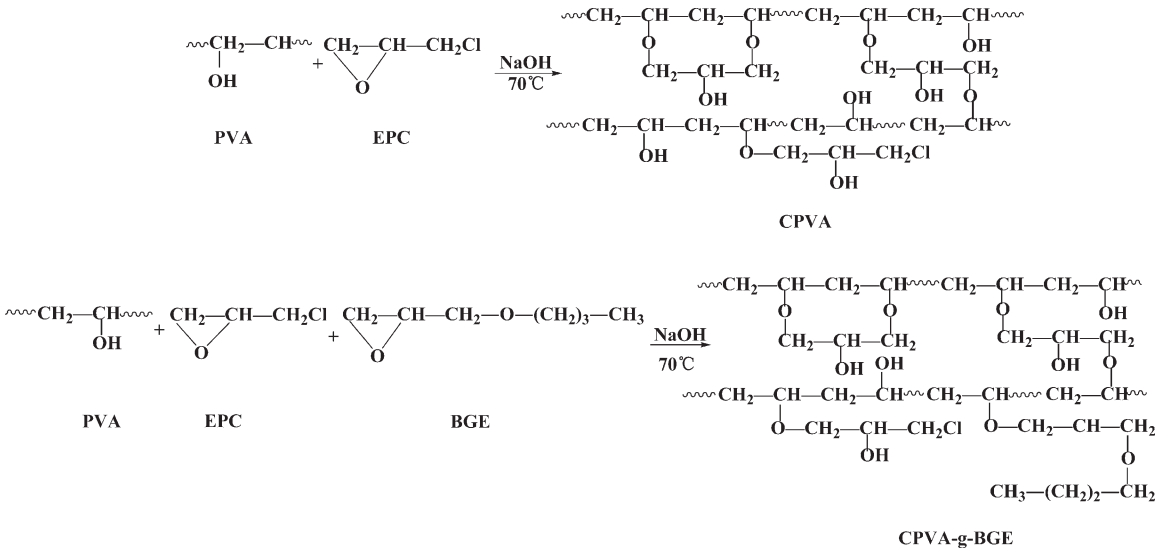

Scheme 1. Synthesis of CPVA and CPVA-*g*-BGE.

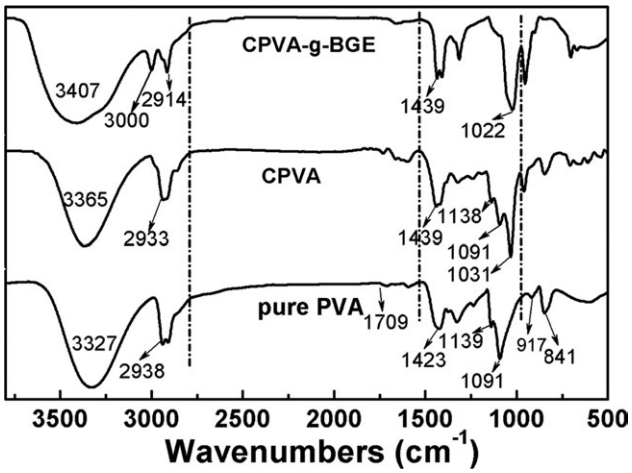

Figure 1. FTIR spectrum of PVA, CPVA, and CPVA-*g*-BGE.

Ink Contact Angle. Ink contact angle on the prepared PVA film was measured by a Krüss DSA30 contact angle goniometer (Germany) at room temperature. The amount of ink droplets used for the measurement was 3.00 μL and the contact angles were measured at five different points.

RESULTS AND DISCUSSION

Structure and Composition of CPVA-*g*-BGE

CPVA and CPVA-*g*-BGE were prepared through the addition reaction of epoxy group of EPC or BGE with the hydroxyl group of PVA, and the reaction formulas were shown in Scheme 1.

The structure of CPVA-*g*-BGE was confirmed by comparison of FTIR spectra with that of PVA and CPVA, as shown in Figure 1. For the sample of virgin PVA, the wide band around 3327 cm^{-1} was attributed to the presence of hydroxyl groups (—OH), the absorption bands at 2938 and 1423 cm^{-1} were attributed to dissymmetrical stretching vibration and the symmetry bending vibration of (—CH_2—), the weak absorption band at 1709 cm^{-1} was attributed to the characteristic absorption peak of ester carbonyl (C=O) due to residual acetate groups during manufacture of PVA from hydrolysis of polyvinyl acetate,[15] the absorption band at 1139 and 1091 cm^{-1} corresponded to (C—O) stretching vibration of crystalline and amorphous phase of PVA,[16] and the absorption bands at 917 and 841 cm^{-1} were assigned to skeletal vibrations of PVA,[17] which were all the characteristic absorptions of PVA.

Comparing the FTIR spectra of CPVA with that of pure PVA, formation of ether linkage (C—O—C) by the reaction of PVA and EPC was evidenced by a peak at 1031 cm^{-1}. In the case of CPVA-*g*-BGE, a new peak at 3000 cm^{-1} can be observed, which was attributed to the characteristic absorption of asymmetric stretching vibration of (—CH_3). Use the peak at 1439 cm^{-1} attributed to the bending vibration of (—CH_2) as the internal standard, the absorption band at 1022 cm^{-1} attributed to the ether linkage (C—O—C) was strengthened, while the absorption band at 1139 and 1091 cm^{-1} attributed to (C—O) stretching vibration were weakened. The result indicated that relatively more ether linkages were formed through the reaction of PVA with BGE, and BGE has been grafted onto the molecular chain of PVA successfully.

Figure 2 shows the ^{1}H NMR spectra of CPVA and CPVA-*g*-BGE in D_2O at room temperature. It can be seen that NMR absorption peak of hydroxyl hydrogen on PVA chain disappeared because the active hydrogen was exchanged by heavy water. The protons in methenyl group (H_b) connected to hydroxyl groups were exhibited at 3.6–4.1 ppm, overlapping with the methenyl group ($H_{b'}$) and methylene group (H_c) produced by ring opening reaction.[18] The protons in the methylene group on the PVA backbone (H_a) and the grafting BGE chain ($H_{a'}$) could be found at 1.5–1.9 ppm. The absorption peak at 0.95 ppm was ascribed to the protons in the methyl group (H_d), which belonged to the

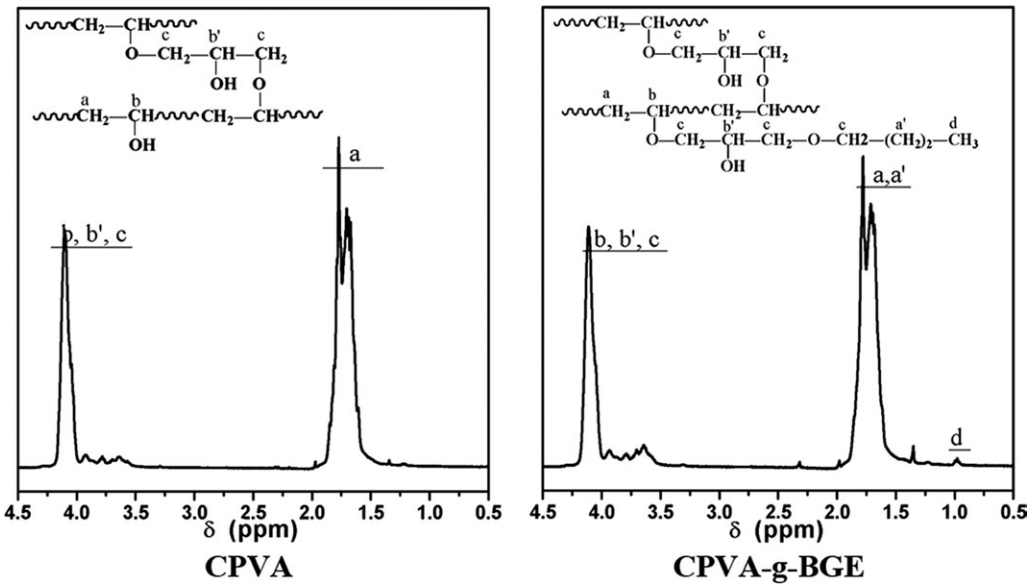

Figure 2. ^{1}H NMR spectrum of CPVA and CPVA-*g*-BGE.

Applied Polymer SCIENCE

Table I. ^{1}H NMR Results of CPVA and CPVA-*g*-BGE with Varying Grafting Ratio of BGE

Samples	δ (ppm)	Type of H	Number of H	Integration area Si	Grafting ratio (%)
CPVA	0.95	H_d	3	0	-
	1.5-1.9	$H_{a\text{-}a'}$	2	64.92	
CPVA/8.8 wt % BGE	0.95	H_d	3	0.57	0.58
	1.5-1.9	$H_{a\text{-}a'}$	2	66.45	
CPVA/17.6 wt % BGE	0.95	H_d	3	1.07	1.06
	1.5-1.9	$H_{a\text{-}a'}$	2	67.82	
CPVA/26.3 wt % BGE	0.95	H_d	3	0.87	0.81
	1.5-1.9	$H_{a\text{-}a'}$	2	72.44	

grafting BGE chains, which further confirmed that the long alkyl chain has been indeed grafted onto the molecular chain of PVA.

The grafting ratio of CPVA-*g*-BGE with different dosages of BGE could be calculated based on the signal intensities of the aforementioned methylene resonance at 1.5–1.9 ppm and methyl peak at 0.95 ppm.[19,20] The grafting ratio of CPVA-*g*-BGE is given by:

$$\text{Grafting ratio} f = I_{\text{Hd}}/(1.5I_{\text{Ha}-a'} - 2\ I_{\text{Hd}})$$

where $I_{\text{Ha-a'}}$ and I_{Hd} are the intensities of the signals at 1.5–1.9 ppm and 0.95 ppm, respectively. The peak intensity of the methyl on the grafting BGE chain was used to calculate the amount of methylene on the BGE chains. The results were presented in Table I.

As shown in Table I, with increasing dosage of BGE, the actual grafting ratio of BGE first increased and then decreased. For 17.6 wt % of dosage of BGE, the grafting ratio reached maximum of 1.06 mol %. Further increasing BGE dosage led to the high monomer concentration and high viscosity of reaction system, which were disadvantage for the monomer to reach PVA chains.

Mechanical Properties of CPVA-*g*-BGE

CPVA and CPVA-*g*-BGE films were prepared by solution evaporation process in order to investigate the mechanical properties. Figure 3 shows the tensile stress–strain curves of CPVA and CPVA-*g*-BGE with varying grafting ratio of BGE. All the samples all presented strain hardening behavior with no yield point and the stress–strain curves exhibited elastic deformation stress plateau, presenting the characteristic of ductile fracture. By grafting with BGE, the strain of CPVA increased remarkably. For the sample with 1.06 mol % of BGE grafting ratio, the area of the stress–strain curves increased significantly, indicating of increasing toughness of CPVA.

The mechanical properties of CPVA-*g*-BGE samples as a function of grafting ratio of BGE were shown in Figure 4. It can be seen that the elongation at break of CPVA-*g*-BGE increased with increasing grafting ratio of BGE, and can reach as high as 899.7% at the highest grafting ratio of BGE (1.06 mol %) with little drop of the tensile strength, while the elongation at break

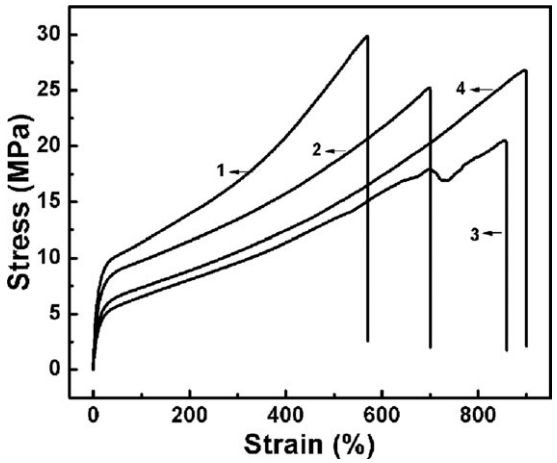

Figure 3. Tensile stress–strain curves of CPVA and CPVA-*g*-BGE with varying grafting ratio of BGE (Grafting ratio: 1 : 0; 2 : 0.58%; 3 : 0.81%; 4 : 1.06%).

of CPVA was 592.7%. Although the hydrogen bonding between molecular chains of PVA was weakened by grafting with alkyl chains, appropriate intermolecular association of alkyl chains facilitated the formation of physical entanglement of molecular chains to strengthen and toughen the PVA matrix.

The deduction about toughening mechanisms could be confirmed by morphologies of tensile fracture surface of samples of CPVA and CPVA-*g*-BGE, as shown in Figure 5.[21–22] Both of them exhibited rough ductile fractured surface, while more folds can be observed for CPVA-*g*-BGE. Large scale of plastic deformation was produced before specimen failure, which is responsible for the necking formation and increase of elongation at break.

Dynamic Mechanical Properties of CPVA-*g*-BGE

DMA has been used to ascertain the viscoelastic performance of materials under stress at different temperatures. *E*' (storage modulus) represents storage capacity of the elastic deformation energy of the materials. *E*'' (loss modulus) can be used to measure the characteristic temperatures matched with various relaxation processes.[23]

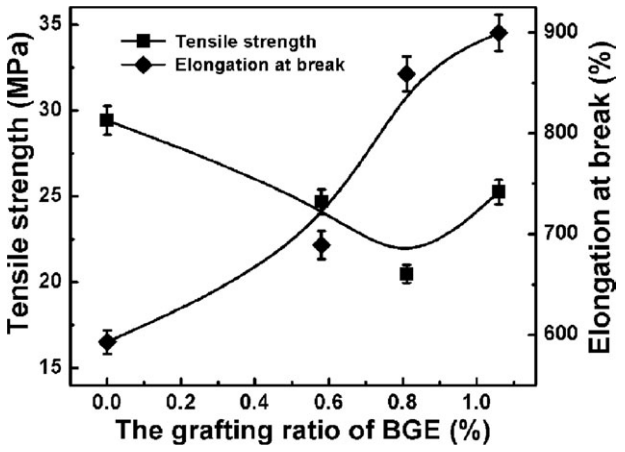

Figure 4. Tensile properties of CPVA-*g*-BGE as a function of grafting ratio of BGE.

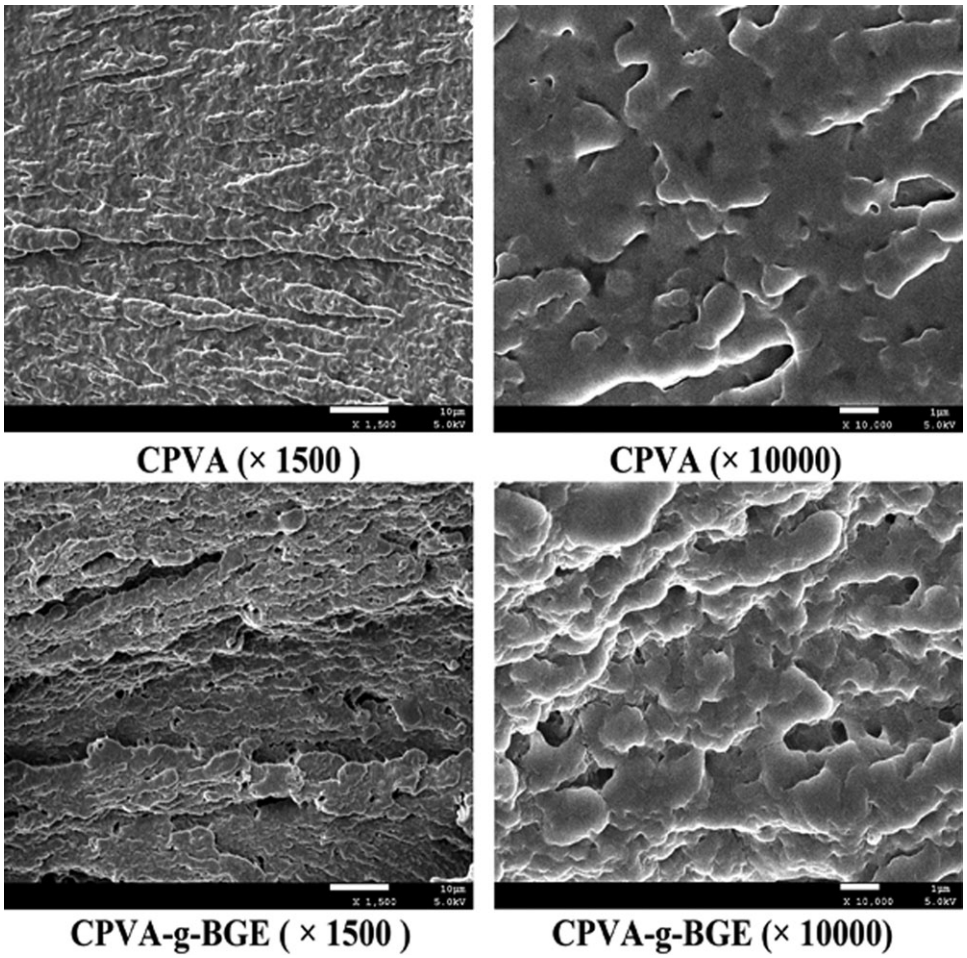

Figure 5. SEM images of CPVA and CPVA-*g*-BGE.

Figure 6 displays typical DMA curves of modulus versus temperature for samples of CPVA-*g*-BGE with varying grafting ratio of BGE. It can be seen that the storage modulus and loss modulus of all samples decreased with increasing temperature, and above 10°C, the decreasing trend became slow. Especially with increasing grafting ratio of BGE, the modulus of CPVA-*g*-BGE first decreased and then quickly increased for the sample with 1.06 mol % grafting ratio of BGE, which was consistent with the result of mechanical strength.

The loss modulus of CPVA in Figure 6(b) showed one relaxation peak at −59.84°C, which should be ascribed to the α-relaxation arising from the chain segmental motion of the molecules in the amorphous regions and corresponded to the glass transition temperature (T_g) of CPVA.[24,25] In the case of CPVA-*g*-BGE, the relaxation peak shifted to low temperature with increasing grafting ratio of BGE. The T_g data were given by Table II. The weakening of the intramolecular and intermolecular hydrogen bonding of PVA and introduction of flexible alkyl chain onto the molecular chain would be responsible for the decrease of T_g.

Nonisothermal Crystallization Property of CPVA-*g*-BGE

It is well known that the crystallization behavior of semicrystalline polymers plays a significant role in determining their mechanical properties. The DSC thermograms of CPVA-*g*-BGE samples with varying grafting ratio of BGE were shown in Figure 7. It can be seen that all samples of CPVA-*g*-BGE had a relatively small and broad melting peak in comparison with that of CPVA. The data were given in Table III.

For CPVA, the melt endothermic peak temperature (T_m) and crystallization exothermic peak temperature (T_c) appeared around 224.5 and 188.1°C, respectively. By grafting with BGE, T_m, T_c, and crystallinity of CPVA-*g*-BGE decreased, and the half peak width and the degree of undercooling ($\Delta T_c = T_m - T_c$) of CPVA increased, indicating of the weakening of crystallization ability of PVA. Introduction of alkyl chain not only reduced the symmetry of molecules of CPVA, but also hindered molecule segments to align into the crystal lattice.[23] However, with increasing grafting ratio of BGE, the crystallization property was improved slightly.

Surface Property of CPVA-*g*-BGE

Figure 8 shows the ink contact angle of CPVA and CPVA-*g*-BGE with varying grafting ratio of BGE. It can be seen that ink contact angles of CPVA-*g*-BGE decreased with increasing grafting ratio of BGE, indicating that introduction of alkyl chain onto the backbone of PVA resulted in the increase of compatibility of CPVA with ink because of its hydrophobicity. This property was advantageous for PVA to be used as surface sizing agent in papermaking.

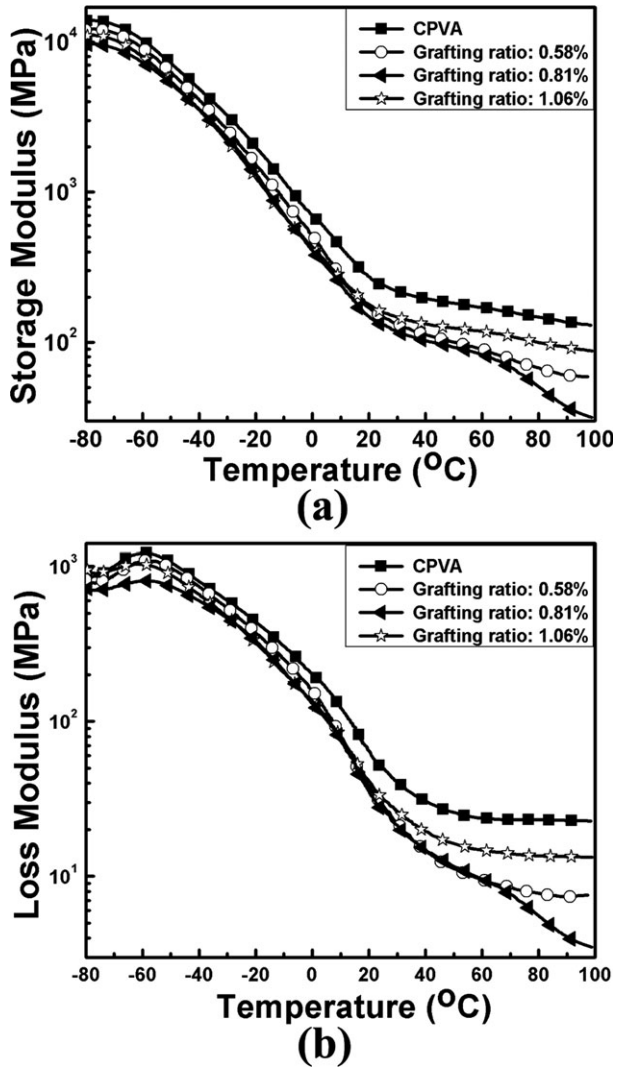

Figure 6. Temperature dependence of (a) storage modulus (b) loss modulus of CPVA-*g*-BGE as a function of grafting ratio of BGE.

Table II. The Glass Transition Temperature of CPVA-*g*-BGE Determined by E''

Grafting ratio (%)	0	0.58	0.81	1.06
T_g (°C)	−59.84	−57.83	−58.81	−61.87

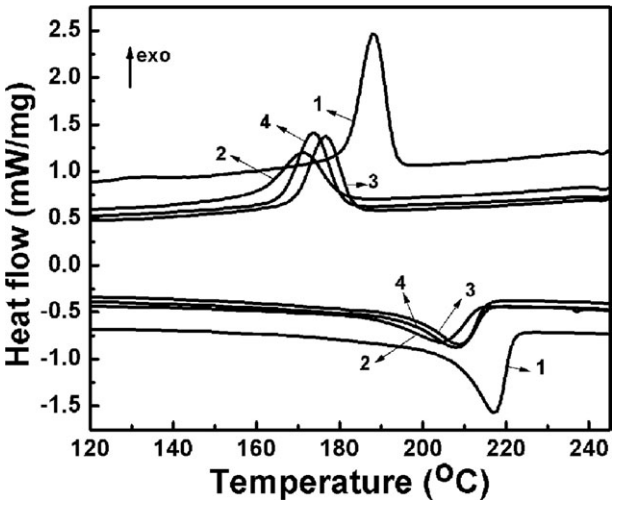

Figure 7. DSC curves of CPVA and CPVA-*g*-BGE with varying grafting ratio of BGE. (Grafting ratio: 1 : 0; 2 : 0.58%; 3 : 0.81%; 4 : 1.06%).

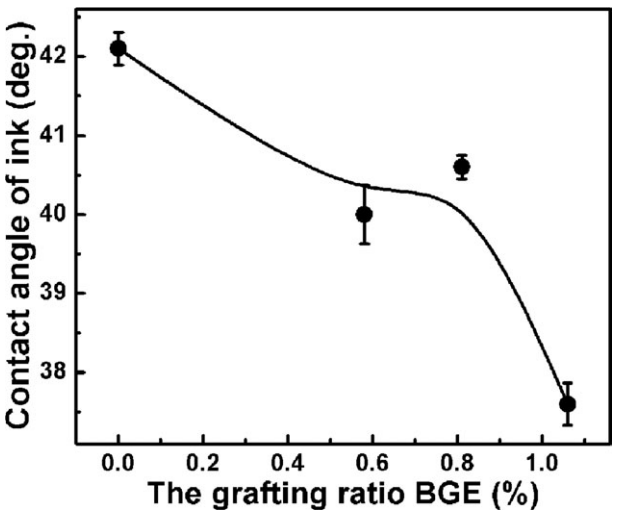

Figure 8. Ink contact angles of CPVA-*g*-BGE as a function of grafting ratio of BGE.

CONCLUSION

The crosslinked alkyl chain grafted CPVA (CPVA-*g*-BGE) was prepared through the addition reaction of epoxy group of BGE with the hydroxyl group of PVA. The structure and property were investigated. It was found that BGE has been grafted onto

Table III. Nonisothermal Crystallization Parameters of CPVA and CPVA-*g*-BGE with Varying Grafting Ratio of BGE

Grafting ratio (%)	T_m (°C)	T_{cOnset} (°C)	T_c (°C)	T_{cEnd} (°C)	X_c (%)	T_m–T_c (°C)	ΔW (°C)
0	217.6	181.8	188.1	193.2	30.65	29.5	6.7
0.58	204.3	160.0	171.2	180.3	20.73	33.1	11.6
0.81	208.7	169.1	176.6	182.9	23.51	32.1	8.2
1.06	208.0	165.8	173.6	180.6	23.81	34.4	8.7

T_m, the melt peak temperature; T_{cOnset}, the onset crystallization temperature; T_c, the crystallization peak temperature; T_{cEnd}, the end crystallization temperature; X_c, the crystallinity; ΔT_c, the degree of undercooling (T_m–T_c), ΔW, the crystalline half-peak width.

the molecular chain of PVA successfully. By grafting with BGE, the area of the stress–strain curves increased, and the elongation at break of CPVA-*g*-BGE increased remarkably with little drop of the tensile strength. SEM observation showed that when compared with PVA, the fractured surface of CPVA-*g*-BGE was much more rough with folds, indicating of increasing toughness of CPVA. The relaxation peak corresponding to the glass transition temperature (T_g) of CPVA shifted to low temperature with increasing grafting ratio of BGE. T_m, T_c, and crystallinity of CPVA decreased when grafting with BGE, indicating of the weakening of crystallization ability. Ink contact angles of CPVA-*g*-BGE decreased with increasing grafting ratio of BGE, indicating the increasing compatibility of CPVA with ink, which was advantageous for PVA to be used as surface sizing agent in papermaking.

REFERENCE

1. Lee, J. S.; Choi, K. H.; Ghim, H. D.; Kim, S. S.; Chun, D. H.; Kim, H. Y.; Lyoo, W. S. *J. Appl. Polym. Sci.* **2004**, *93*, 1638.
2. Yang, E.; Qin, X.; Wang, S. *Mater. Lett.* **2008**, *62*, 3555.
3. Belder, D.; Deege, A.; Husmann, H.; Kohler, F.; Ludwig, M. *Electrophoresis* **2001**, *22*, 3813.
4. Kaboorani, A.; Riedl, B. *Compos. Part A Appl. Sci.* **2011**, *42*, 1031.
5. Street, P. C. U.S. Pat.4,333,795 (**1982**).
6. Feng, S.-S.; Huang, G. *J. Controlled Release* **2001**, *71*, 53.
7. Moreira, A. B. R.; Perez, V. H.; Zanin, G. M.; Castro, H. F. *Energy Fuels* **2007**, *21*, 3689.
8. Qin, X.-H.; Wang, S.-Y. *J. Appl. Polym. Sci.* **2008**, *109*, 951.
9. Takano, T.; Fukuda, M.; Satake, T.; Taniguchi, M. U.S. Pat.6,013,359. (**2000**).
10. Yang, C. Q.; Xu, G. U.S. Pat.6,379,499 (**2002**).
11. Ibrahim, M. M.; Mobarak, F.; El-Din, E. I. S.; Ebaid, A. E.-H. E.; Youssef, M. A. *Carbohydr. Polym.* **2009**, *75*, 130.
12. Chang, M.-H.; Kim, B. C. *Macromol. Symp.* **2007**, *249–250*, 591.
13. Coleman, J. N.; Cadek, M.; Blake, R.; Nicolosi, V.; Ryan, K. P.; Belton, C.; Fonseca, A.; Nagy, J. B.; Gun′ko, Y. K.; Blau, W. J. *Adv. Funct. Mater.* **2004**, *14*, 791.
14. Ding, B.; Kim, H.-Y.; Lee, S.-C.; Lee, D.-R.; Choi, K.-J. *Fiber. Polym.* **2002**, *3*, 73.
15. Sreedhar, B.; Chattopadhyay, D. K.; Karunakar, M. S. H.; Sastry, A. R. K. *J. Appl. Polym. Sci.* **2006**, *101*, 25.
16. Sugiura, K.; Hashimoto, M.; Matsuzawa, S.; Yamaura, K. *J. Appl. Polym. Sci.* **2001**, *82*, 1291.
17. Wang, H.-L.; Fernandez, J. E. *Macromolecules* **1993**, *26*, 3336.
18. Amiya, S.; Tsuchiya, S.; Qian, R.; Nakajima, A. *Pure Appl. Chem.* **1990**, *62*, 2139.
19. Aoi, K.; Aoi, H.; Okada, M. *Macromol. Chem. Phys.* **2002**, *203*, 1018.
20. Chen, S.-C.; Wang, X.-L.; Yang, K.-K.; Wu, G.; Wang, Y.-Z. *J. Polym. Sci. A: Polym. Chem.* **2006**, *44*, 3083.
21. Yu, F.; Liu, T.; Zhao, X.; Yu, X.; Lu, A.; Wang, J. *J. Appl. Polym. Sci.* **2012**, *125*, E99.
22. Zhen, W.; Lu, C. *Appl. Surf. Sci.* **2012**, http://dx.doi.org/10.1016/j.apsusc.2012.03.145.
23. Wang, J.; Ye, L. *Polym. Int.* **2012**, *61*, 571.
24. Zhen, W.; Lu, C.; Li, C.; Liang, M. *Appl. Clay. Sci.* **2012**, *57*, 64.
25. Wang, J.; Wang, K.; Ye, L. *J. Thermoplast. Compos.* **2011**, *24*, 97.